Chapter 5

Entropy change at the first-order magnetostructural transition in $Gd_5(Si_xGe_{1-x})_4$

5.1 Introduction

In this chapter we present a detailed analysis of the different contributions to the entropy change arising from the application of a magnetic field at a first-order field-induced transition, in order to account for the discrepancies discussed in section 2.7 [1, 2, 3, 4, 5, 6]. For this purpose, magnetisation isotherms in $Gd_5(Si_xGe_{1-x})_4$ for $0 \leq x \leq 0.5$ (compositional range in which the first-order magnetostructural transition takes place) were measured up to very high fields (~23 T). The values of the entropy change obtained from the Clausius-Clapeyron equation (Eq. 1.17) and the Maxwell relation (Eq. 1.6) are compared and analysed within the framework of a simple phenomenological model based on the temperature and field dependence of the magnetisation. Calorimetric measurements of the transition entropy change were also carried out on $Gd_5(Si_xGe_{1-x})_4$ series of alloys, by using the high-sensitivity differential scanning calorimeter under magnetic field described in Chapter 4. Results are compared to those obtained from indirect approaches through magnetisation measurements.

5.2 Magnetisation measurements

Magnetisation measurements were performed at the Grenoble High Magnetic Field Laboratory. $M(H)$ curves were recorded up to 23 T, both under increasing and decreasing H, from 4.2 to 310 K with a temperature step of 3 to 5 K. The following samples were measured: x=0 (#1, as-cast), x=0.05 (#1, T4+Q treat-

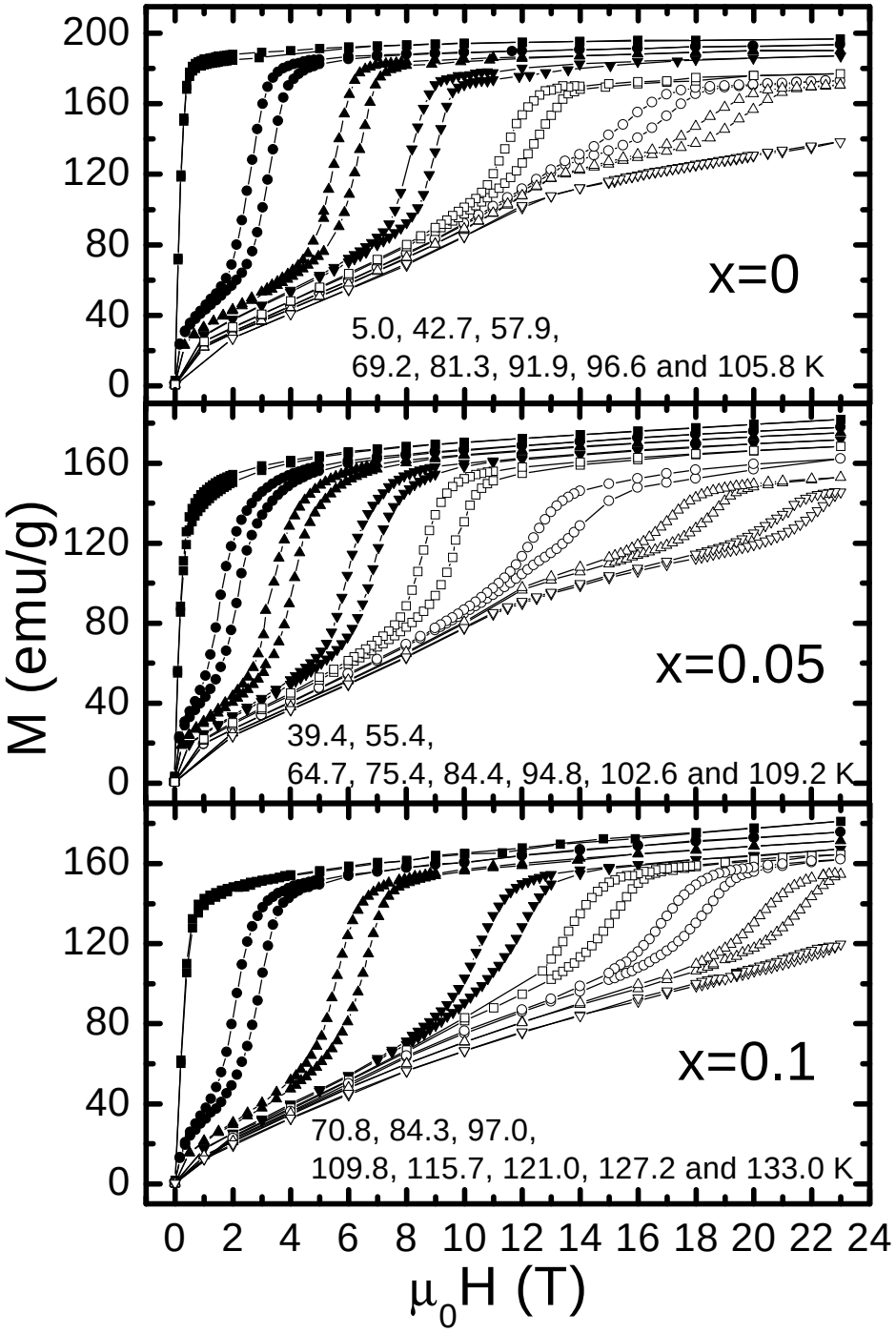

Figure 5.1: Selected magnetisation isotherms of $Gd_5(Si_xGe_{1-x})_4$ for x=0, 0.05 and 0.1 under increasing and decreasing field. Temperatures labeled for each composition refer to isotherms from top/left to bottom/right.

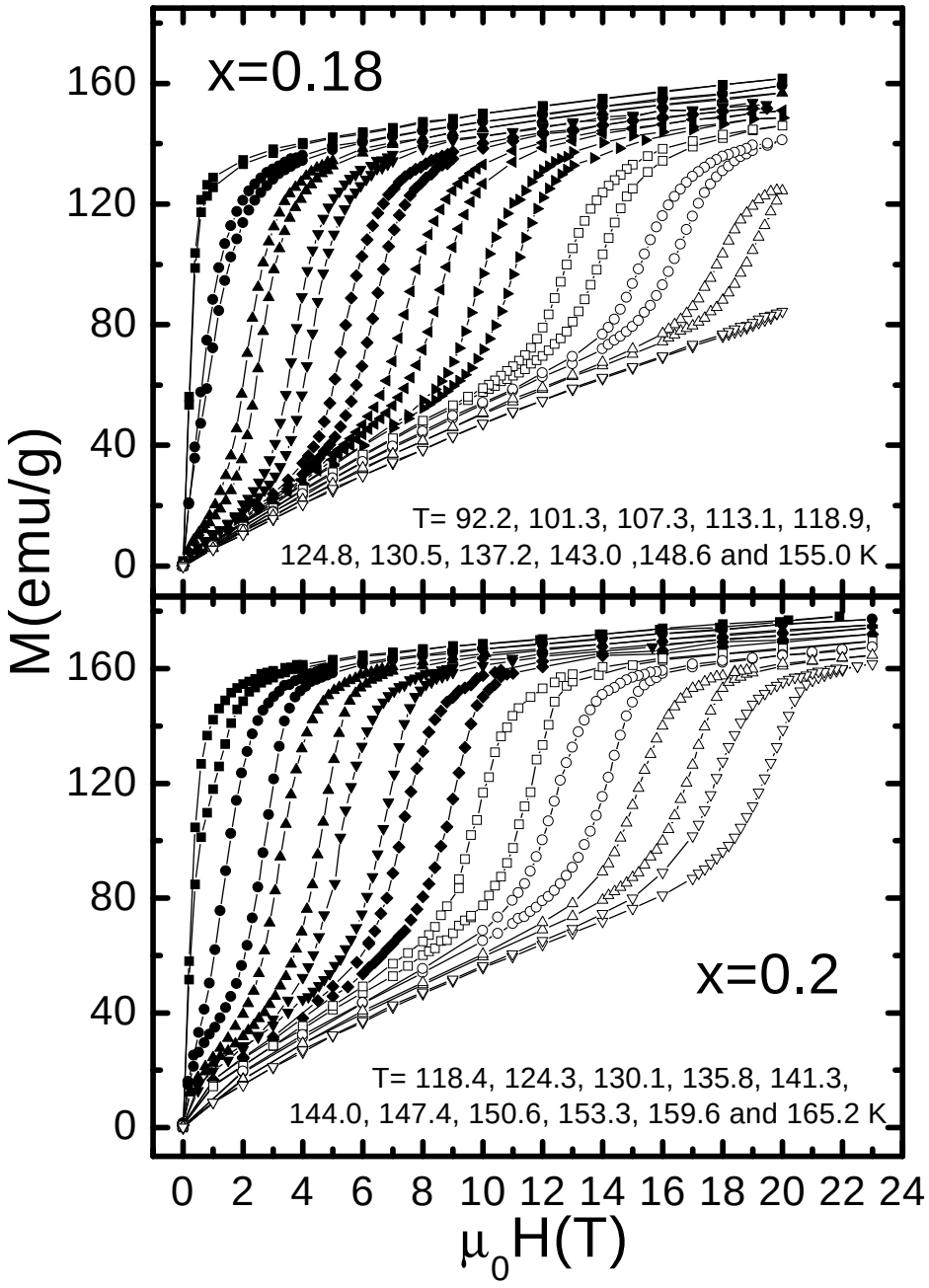

Figure 5.2: Selected magnetisation isotherms of $Gd_5(Si_xGe_{1-x})_4$ for x=0.18 and 0.2 under increasing and decreasing field. Temperatures labeled for each composition refer to isotherms from top/left to bottom/right.

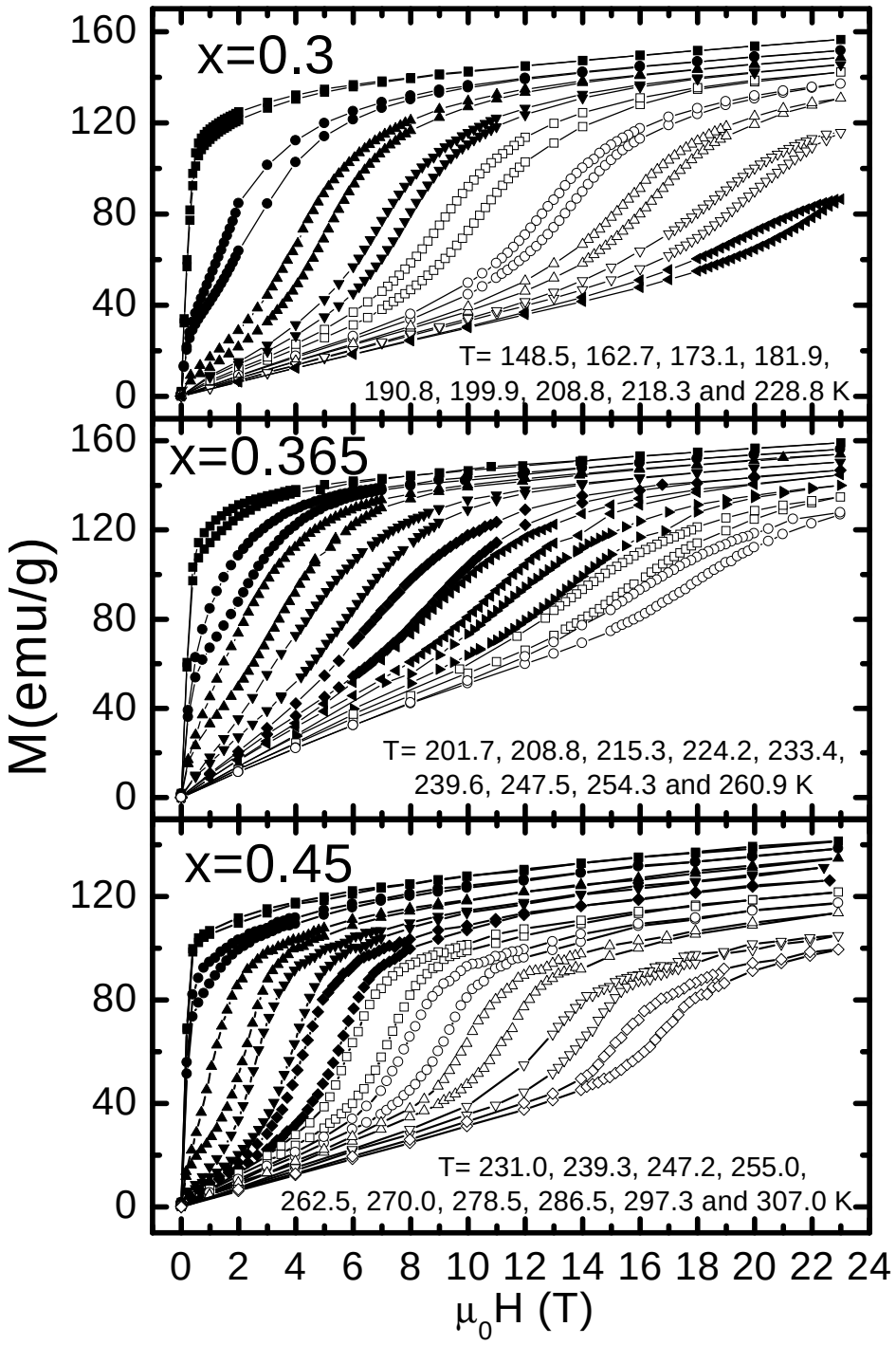

Figure 5.3: Selected magnetisation isotherms of $Gd_5(Si_xGe_{1-x})_4$ for x=0.3, 0.365 and 0.45 under increasing and decreasing field. Temperatures labeled for each composition refer to isotherms from top/left to bottom/right.

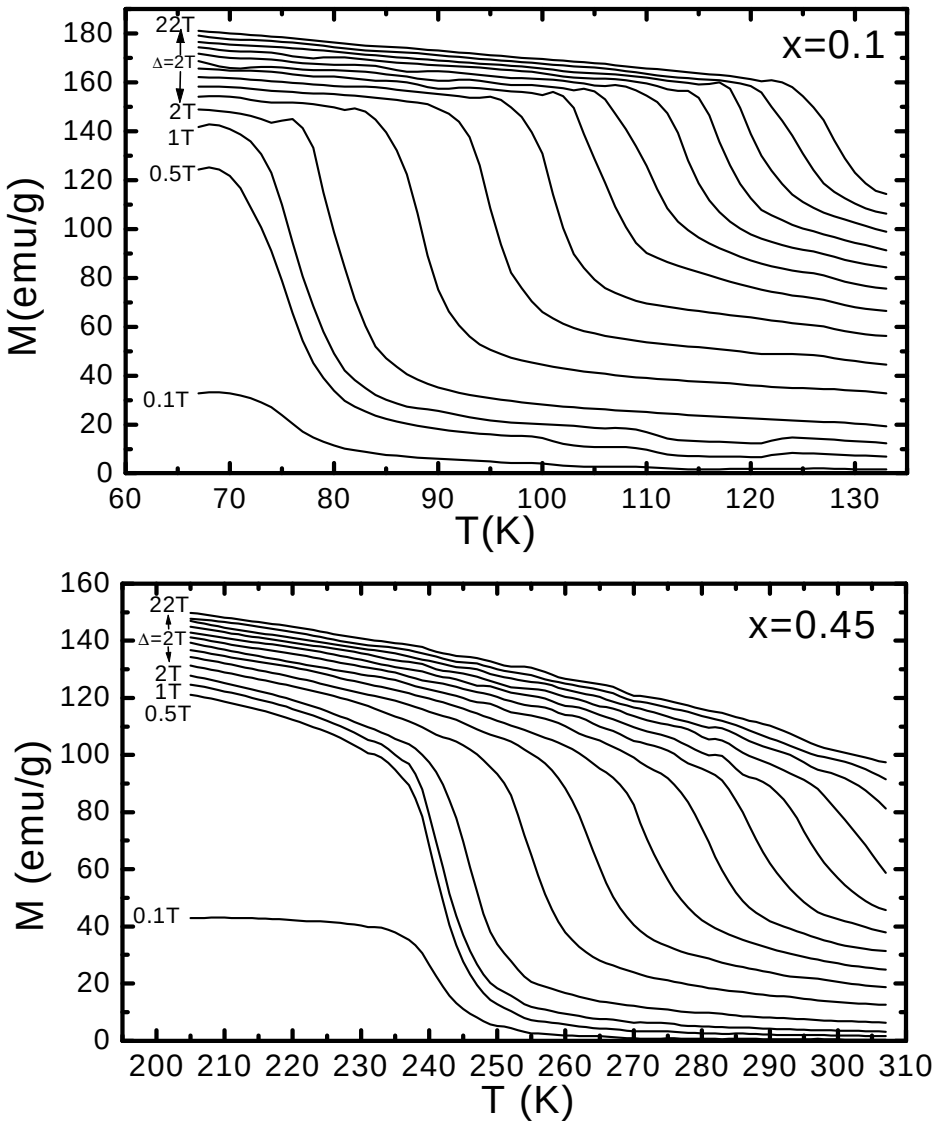

Figure 5.4: Magnetisation as a function of temperature under selected applied fields (0.5, 1, 2, 4, 6, 8, 10, 12, 14, 16, 18, 20 and 22 T) for x=0.1 and x=0.45 compounds, taken from $M(H)$ data for increasing field.

ment), x=0.1 (#1, as-cast), x=0.18 (#1, T4 treatment), x=0.2 (#1, as-cast), x=0.3 (#2, T4+Q treatment), x=0.365 (#3, as-cast) and x=0.45 (#7, T4 treatment).

$M(H)$ isotherms are shown in Fig. 5.1 (x=0, 0.05 and 0.1), Fig. 5.2 (x=0.18 and 0.2) and Fig. 5.3 (x=0.3, 0.365 and 0.45). These curves exhibit a jump ΔM at the magnetostructural transition [1, 2, 7, 8], which spreads over a field range ΔH_t (~2-4 T for $0 \leq x \leq 0.2$ samples and ~4-6 T for $0.24 \leq x \leq 0.5$ compounds). The hysteresis in the transition reveals its first-order nature. The transition field, H_t, for increasing and decreasing applied field is defined for each isotherm as the field corresponding to the inflection point within the transition region. We note that the application of a field of 23 T enables the observation of the transition at temperatures of up to ~80 K above $T_t(H = 0)$. The variation of H_t with T is linear for $0.24 \leq x \leq 0.5$ compounds, while the slope dH_t/dT_t changes within two limiting values for $0 \leq x \leq 0.2$ alloys. The detailed study of $H_t(T)$ for all compositions is presented in Chapter 7. The change in the slope of the $M(H)$ curves observed in Fig. 5.1 for x=0 and 0.05 above ~90 K and ~12 T corresponds to a nonreported magnetic transition appearing at very high fields, which is studied in Chapter 8. For the compounds from x=0 to x=0.2 (Figs. 5.1 and 5.2), the first-order field-induced transition occurs from AFM to FM phases, while for the rest of compounds (from x=0.3 to x=0.45, see Fig. 5.3) it occurs from PM to FM phases. This difference is observed in ΔM, which is more abrupt for the AFM-FM transition. Figure 5.4 shows the magnetisation data (for increasing field) displayed as a function of T at constant magnetic field for x=0.1 and x=0.45 compounds, as paradigmatic examples of Ge-rich and intermediate compostional regions, respectively.

5.3 DSC measurements

DSC data under different magnetic fields (0 to 5 T) were measured for the following samples: x=0 (#1, as-cast), x=0.05 (#1, T4+Q treatment), x=0.1 (#1, as-cast), x=0.18 (#1, T4 treatment), x=0.2 (#1, as-cast), x=0.25 (#2, as-cast), x=0.3 (#2, as-cast), x=0.365 (#3, as-cast) and x=0.45 (#7, T4 treatment). Measurements were carried out by scanning T at constant magnetic fields, since the availabe range in temperature is larger than the available range in H. In these measurements, first-order transitions give rise to a large peak in thermal curves (dQ/dT). Second-order transitions are observed as small λ-type jumps in the dQ/dT baseline. The shape of the thermal curves for all compositions with $x \leq 0.2$ reveals the first-order nature of the low-temperature AFM-FM transition and the second-order nature of the high-temperature PM-AFM transition (see Fig. 5.5 for x=0, 0.05 and 0.2, Fig. 5.6 for x=0.18, where the second-order transitions are labeled, and Fig. 4.7 in Chapter 4 for x=0.1). For the rest of compositions ($0.24 \leq x \leq 0.5$),

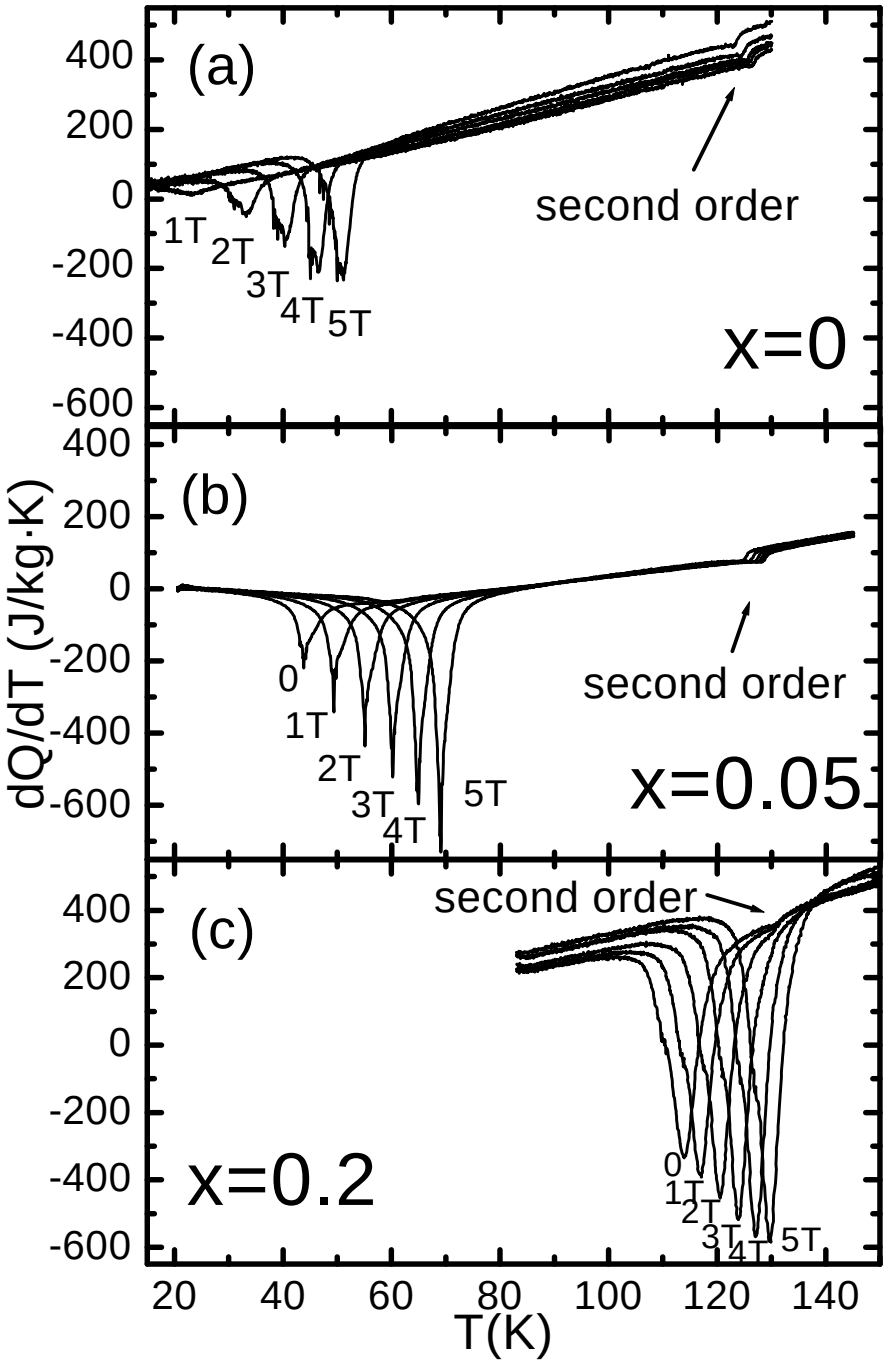

Figure 5.5: DSC data on cooling at selected applied fields up to 5 T for $Gd_5(Si_xGe_{1-x})_4$: (a) x=0, (b) x=0.05 and (c) x=0.2. The second-order transition is labeled for each composition.

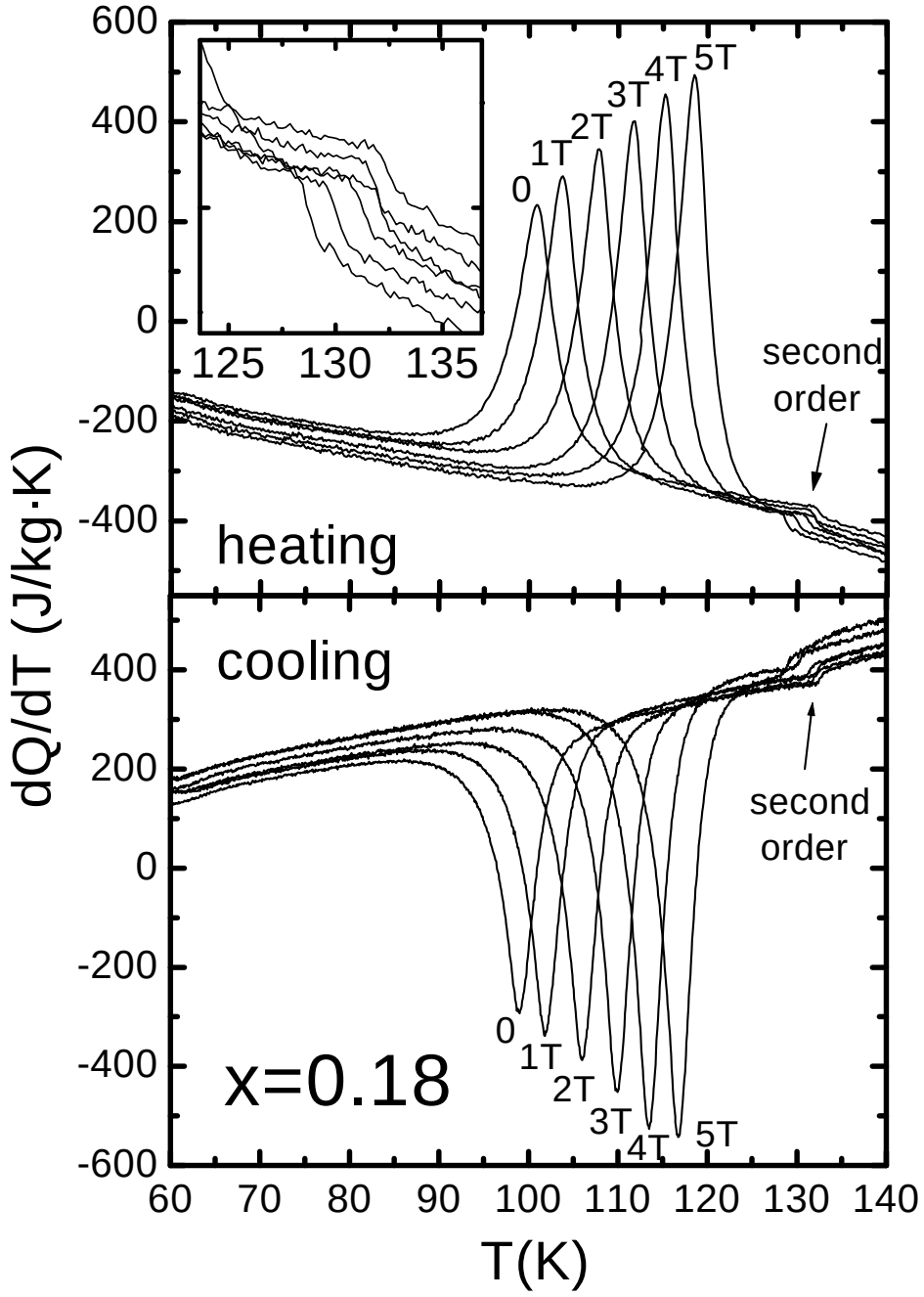

Figure 5.6: DSC data for x=0.18 on heating and cooling the sample under H. Inset: Detail of the second-order transition on heating, from 0 (top) to 5 T (bottom).

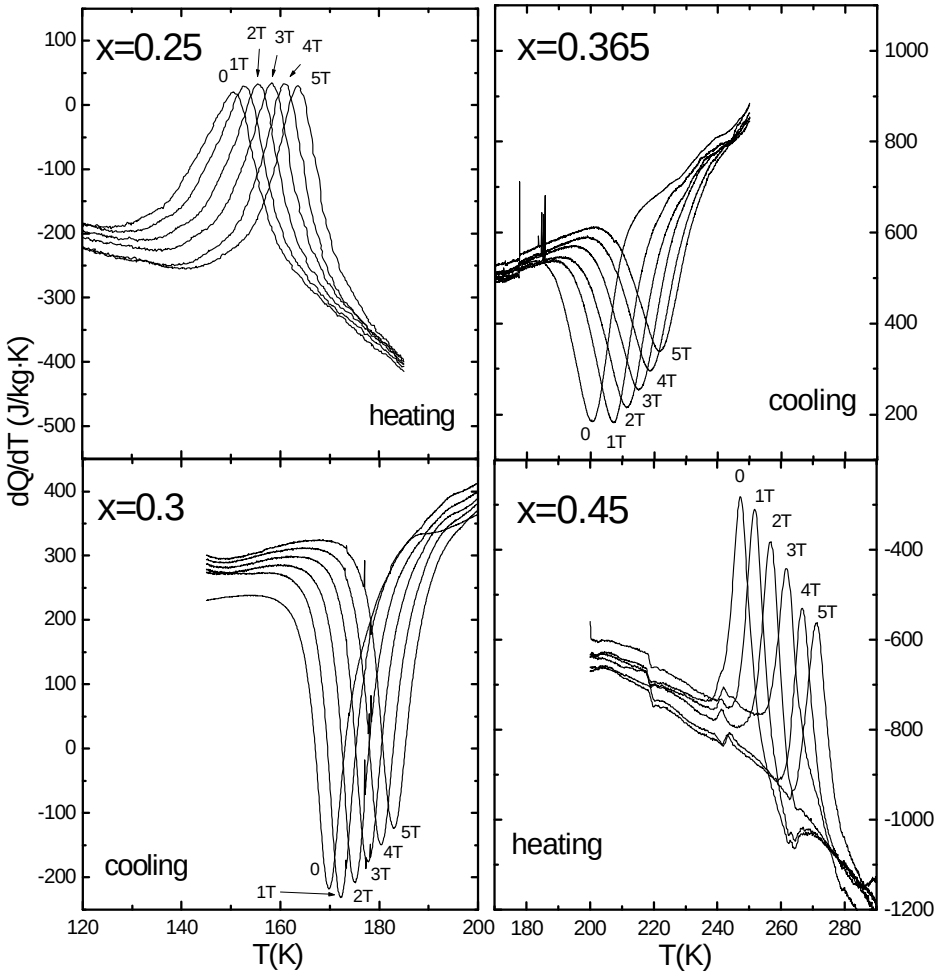

Figure 5.7: DSC data at selected applied fields up to 5 T for x=0.25 (heating), x=0.3 (cooling), x=0.365 (cooling) and x=0.45 (heating).

only one peak is displayed, corresponding to the first-order PM-FM transition (Fig. 5.7 for x=0.25, 0.3, 0.365 and 0.45). For all samples, a hysteresis of 2-4 K between cooling and heating runs is observed, see for example Figs. 5.6 and 4.7. T_t is estimated as the temperature at the maximum of the dQ/dT peak and increases with the applied field (up to 5 T) in all samples. The detailed study of $H(T_t)$ for all compositions is presented in Chapter 7. We note that for x=0, the cooling process at zero field does not show any first-order peak [hence it is not displayed in Fig. 5.5 (a)]. This fact can be explained by taking into account that the FM ground state for x=0 can not be achieved by cooling down to low temperature at zero field, since the sample remains AFM, as discussed in section 2.4.1. The application of a field of ~1 T is needed in order to stabilize the FM phase through an irreversible transition [9, 10, 11]. Fig. 5.5 shows how the first-order transition gets progressively closer to the second-order transition as Si content, x, is increased. In particular, Fig. 5.5 (c) shows how the first-order peak overlaps the second-order jump when a field of ~3 T (or larger) is applied for x=0.2.

5.4 Evaluation of the entropy change

5.4.1 Magnetic and calorimetric evaluations

The entropy change as a function of T for each x may be obtained indirectly from magnetisation data:

(i) On one hand, the entropy change at a first-order transition, ΔS, can be obtained by using the Clausius-Clapeyron equation (Refs. [2, 12] and section 2.7),

$$\Delta S = -\Delta M \frac{dH_t}{dT_t} \ ,$$

where ΔM has been estimated as the difference in the magnetisation at H_t between the linear extrapolations of $M(H)$ well above and below the transition region, and dH_t/dT_t is evaluated from the $H_t(T)$ curve obtained from the magnetisation isotherms. This estimation of ΔM does not consider the variation of M due to the field change (since the transition takes place in a field range ΔH_t), but only due to the first-order phase transition.

(ii) On the other hand, the total entropy change due to the variation of the magnetisation by the application of a magnetic field, $\Delta S(0 \rightarrow H_{max})$, may be evaluated by using the Maxwell relation (Ref. [13] and section 1.2),

$$\Delta S(0 \rightarrow H_{max}) = \int_0^{H_{max}} \left(\frac{\partial M}{\partial T}\right)_H dH \ .$$

This integration is evaluated numerically from magnetisation isotherms. It is straightforward to note that the entropy change at the transition, ΔS, and the total entropy change, $\Delta S(0 \rightarrow H_{max})$, do not necessarily yield the same value.

The entropy change can also be obtained by calorimetry. DSC data enables us to obtain the entropy change (and latent heat) at the first-order transition, after a proper integration of the calorimetric peak (see section 3.2.3 and Chapter 4), as

$$\Delta S = \int_{T_L}^{T_H} \frac{1}{T}\frac{dQ}{dT}dT \ ,$$

where T_H and T_L are respectively temperatures above and below the starting and finishing transition temperatures.

A comparision among all three methods to evaluate the entropy change is shown in Fig. 5.8 for x=0.45 (using increasing H and cooling data), as a good example of the behaviour of the $0.24 \leq x \leq 0.5$ alloys and in Fig. 5.9 for x=0 and 0.05 (using decreasing H and heating data), as a paradigmatic example of the $0 \leq x \leq 0.2$ compounds.

For x=0.45, the entropy change obtained from the Maxwell method is displayed as dashed lines. Different curves of entropy change as a function of T are obtained depending on the maximum applied field, H_{max}. These curves display the typical behavior previously reported [1, 2]: first, a rapid increase at low T, then a maximum value at about $T_t(H = 0)$, followed by a plateau-like behaviour, and finally a sharp decrease at high T. Figure 5.8 also shows the values of the entropy change at the transition, ΔS, obtained from the Clausius-Clapeyron equation for x=0.45 (present data, solid squares) and x=0.5 (taken from Ref. [2], open squares), and DSC data (open triangles) for x=0.45. We note that ΔS obtained from the Clausius-Clapeyron equation and calorimetry yields the same values, within the experimental error. This suggests that both methods actually evaluate the entropy change associated with a first-order transition. The maximum value of the entropy change achieved using the Maxwell relation can be above or below ΔS depending on H_{max}.

For x=0 and 0.05 (Fig. 5.9), the comparision between methods is very similar to that in x=0.45. The values obtained using the Clausius-Clapeyron equation (open squares) agree, within the experimental error, with the calorimetric ones (open triangles), although DSC data give slightly higher values, as observed in some other samples (see section 6.3). This small difference may be related to the fact that the coexistence line in the phase diagram is crossed at different directions, *i.e.*, sweeping H in magnetisation and sweeping T in DSC (see Chapter 9). $\Delta S(0 \rightarrow H_{max})$ calculated from the Maxwell relation (dashed lines) gives different values depending on the maximum applied field, being clearly above ΔS when $H_{max} > \Delta H_t$.

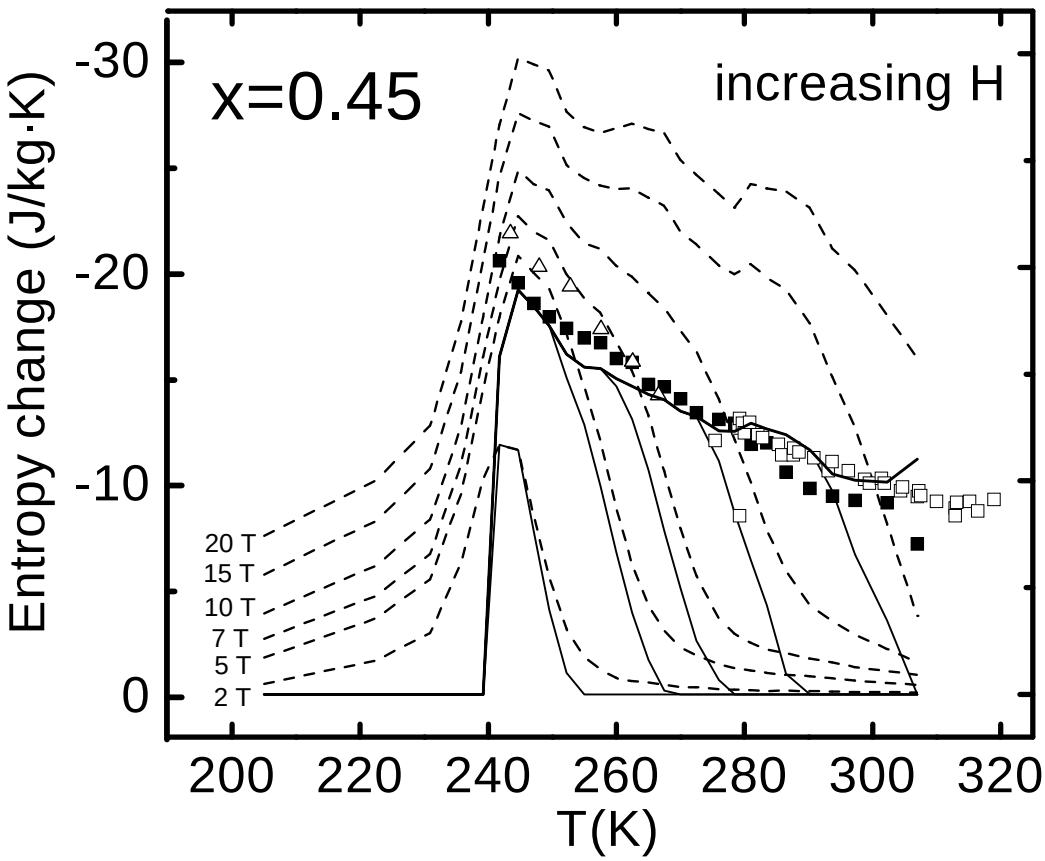

Figure 5.8: Entropy change for $Gd_5Si_{1.8}Ge_{2.2}$ (x=0.45) calculated from: (i) Maxwell relation integrating up to H_{max} (dashed lines), (ii) Clausius-Clapeyron equation (solid squares this work and open squares for x=0.5 from Ref. [2]), (iii) DSC measurements under field (open triangles), and (iv) Maxwell relation integrating within ΔH_t (solid lines). H_{max} is labeled beside each dashed line, and also stands for the solid lines from left to right increasing the field.

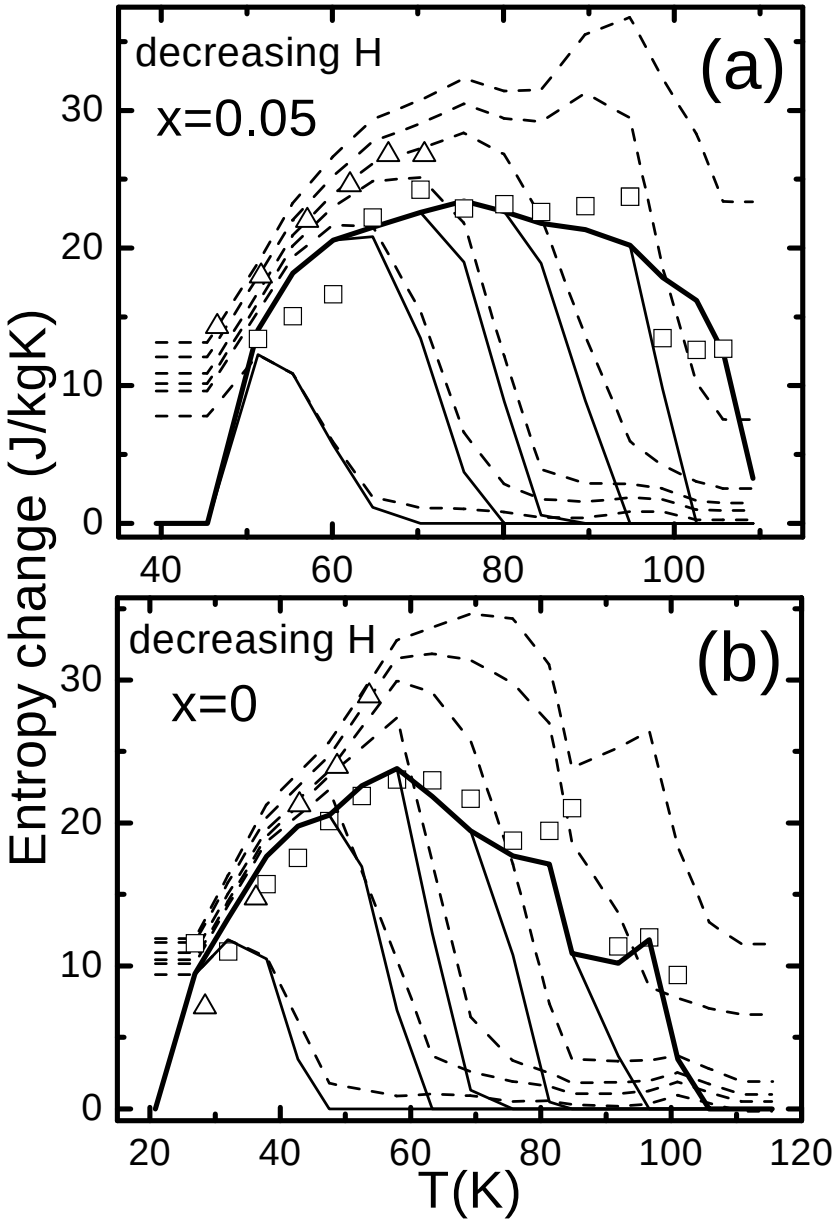

Figure 5.9: Entropy change in $Gd_5(Si_xGe_{1-x})_4$, for (a) x=0.05 and (b) x=0, calculated by using: DSC measurements under field (open triangles); the Clausius-Clapeyron equation (open squares); the Maxwell relation integrating from H_{max} (20, 15, 10, 7, 5 and 2 T, from right to left, respectively) to zero (dashed lines); and the Maxwell relation integrating only within the transition region (solid line).

Besides, $\Delta S(0 \rightarrow H_{max})$ obtained from the Maxwell relation for x=0 and x=0.05 shows a double peak structure, when integrating from very high fields (15 and 20 T) to zero, which evidences the existence of two magnetic transitions in the system. The high-T peak is related to the expected AFM-FM transition, while the low-T peak is associated with a transition from the AFM phase to a phase with short-range antiferromagnetic correlations, which appears in the Ge-rich compounds (see Chapter 8). This effect is also evident in ΔS determined from the Clausius-Clapeyron equation at high T_t, *i.e.*, at very high H_t.

5.4.2 Use of the Maxwell relation within the transition region

The difference between the transition entropy change ΔS obtained from both DSC and the Clausius-Clapeyron approach and $\Delta S(0 \rightarrow H_{max})$ obtained from the Maxwell relation, can be understood by taking into account the fact that the Maxwell method includes the following contributions,

$$\Delta S(0 \rightarrow H_{max}) = \int_0^{H_a} \left(\frac{\partial M}{\partial T}\right)_H dH + \int_{H_a}^{H_b} \left(\frac{\partial M}{\partial T}\right)_H dH + \int_{H_b}^{H_{max}} \left(\frac{\partial M}{\partial T}\right)_H dH \ , \qquad (5.1)$$

with H_a=$H_t - \Delta H_t/2$ and H_b=$H_t + \Delta H_t/2$, being ΔH_t the transition field range. The first and the third integrals yield the entropy change that arises from the field and temperature dependence of the magnetisation in each magnetic phase that the transition involves. Only the second term accounts for the contribution to the entropy change of the magnetostructural transition. This is indicated by the fact that, for x=0.45, the plateau-like behaviour of the solid lines in Fig. 5.8 (computed using the second integral in Eq. 5.1, $\int_{H_a}^{H_b}(\partial M/\partial T)_H dH$) perfectly matches the ΔS values given by the Clausius-Clapeyron equation and by calorimetry. A transition field region of $\mu_0\Delta H_t$ ~4 T has been used, obtained from the high field $M(H)$ curves. Note also that when H_{max} is less than ΔH_t, which is the minimum field needed to complete the transition, the maximum value of $\Delta S(0 \rightarrow H_{max})$ is lower than ΔS (see for instance, the curve corresponding to $\mu_0 H_{max}$ = 2 T in Fig. 5.8). Moreover, for $H_{max} \geq \Delta H_t$, the plateau-like region extends over the temperature range for which $H_{max} \geq H_b(T)$. Consequently, as $H_b(T)$ increases with T, the abrupt decrease from the plateau-like region at higher T is due to the truncation of the second integral at H_{max}.

The same result is plotted as solid lines in Fig. 5.9 for x=0.05 ($\mu_0\Delta H_t$ ~3 T from $M(H)$) and x=0 ($\mu_0\Delta H_t$ ~4 T) samples, showing that $\Delta S(H_a \rightarrow H_b) = \int_{H_a}^{H_b}(\partial M/\partial T)_H dH$ matches the Clausius-Clapeyron value. This suggests that the calculation of the entropy change using the Maxwell relation evaluated within

ΔH_t and using the Clausius-Clapeyron equation, are equivalent for the first-order transition in the whole compositional range of $Gd_5(Si_xGe_{1-x})_4$ alloys.

5.5 Phenomenological models for the entropy change

In order to account for the main features of the entropy change reported in the last section (5.4), we propose a phenomenological model that takes into account the basic features of the magnetisation in a system with a first-order field-induced phase transition. In a first phenomenological approach, only the basic behaviour of the transition is considered, by assuming that $M(T)$ is constant outside the transition region. In the advanced approach, the overall behaviour of the magnetisation is also taken into account by assuming that $M(T)$ is not constant outside the transition region.

5.5.1 First phenomenological approach: $M(T) = \text{const.}$

In this first model, the magnetisation curves are considered to be of the form:

$$M(T,H) = M_0 + \Delta M\, F\left(\frac{T - T_t(H)}{\xi}\right) \quad , \tag{5.2}$$

where M_0 and ΔM are assumed to be T and H independent, and $F(T)$ is a monotonously decreasing function of width ξ such that $F \to 1$ for $T \ll T_t(H)$ and $F \to 0$ for $T \gg T_t(H)$. The case $\xi \to 0$ corresponds to the ideal first-order transition (F is then the Heaviside function). Using the Maxwell relation and assuming a linear field dependence of the transition temperature ($dT_t/dH_t \equiv \alpha$=constant), the entropy change is given by

$$\Delta S\,(0 \to H_{max}) = \Delta S \left[F\left(\frac{T - T_t(H_{max})}{\xi}\right) - F\left(\frac{T - T_t(H=0)}{\xi}\right)\right] \quad , \tag{5.3}$$

where $\Delta S = \Delta M/\alpha$ (the transition entropy change from the Clausius-Clapeyron equation). It is worth stressing that when the transition temperature is not field dependent, $\Delta S\,(0 \to H_{max}) = 0$ irrespective of the value of ΔS. In general, $\Delta S\,(0 \to H_{max})$ is a fraction of the transition entropy change (ΔS), which depends on the magnitude of the shift of T_t with the magnetic field, and reaches its maximum value, ΔS, for high enough applied field. Results are even valid in the limit $\xi \to 0$, for which $\Delta S\,(0 \to H_{max}) = \Delta S$ for all H_{max}.

A simple analytical picture is provided by assuming that F is a linear function of temperature which extends within the temperature range $\Delta T_t = \alpha \Delta H_t = \xi$. Results are shown in Fig. 5.10. The general trends compare very well with results in Figs. 5.8 and 5.9 obtained by integrating the Maxwell relation within the

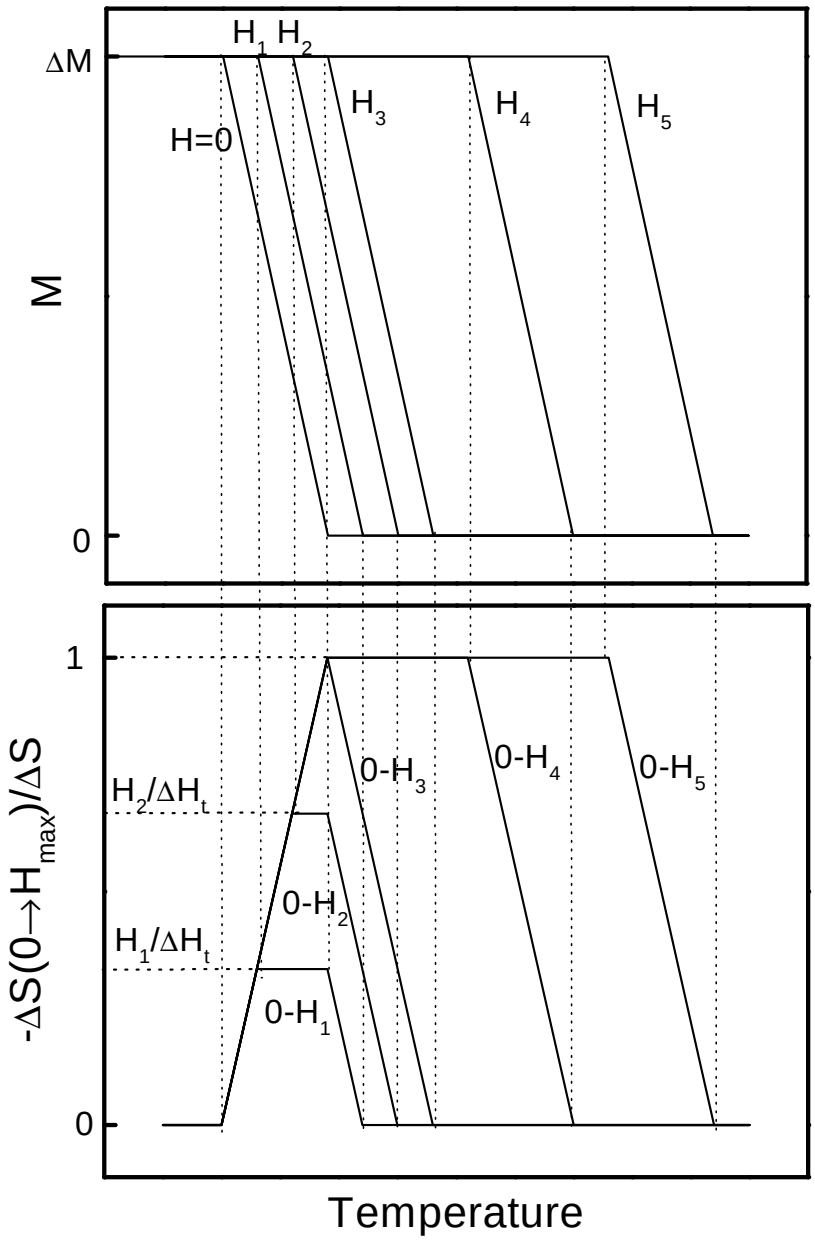

Figure 5.10: Upper panel: temperature dependence of the magnetisation across the transition region at different fields, as described for the first phenomenological model. Lower panel: corresponding entropy change $\Delta S\,(0 \rightarrow H_{max})$ calculated from the Maxwell relation. In this figure, ΔS stands for the entropy change of the transition, obtained from the Clausius-Clapeyron equation.

transition range (second integral of Eq. 5.1, $\Delta S(H_a \rightarrow H_b) = \int_{H_a}^{H_b} (\partial M/\partial T)_H dH$). Note that within the scope of the present model, a true plateau is obtained since ΔM has been assumed to be T-independent, in contrast with the experimental results (Figs. 5.1, 5.2 and 5.3), where ΔM decreases linearly with T. It is also observed that when H_{max} is not high enough to complete the transition ($H_{max} < \Delta H_t$), then $\Delta S(0 \rightarrow H_{max}) = (H_{max}/\Delta H_t)\Delta S$ is smaller than ΔS. Accordingly, $(H_{max}/\Delta H_t)$ is the fraction of the sample that has been transformed. For $H_{max} \geq \Delta H_t$, $\Delta S(0 \rightarrow H_{max})$ reaches its maximum value $\Delta S(0 \rightarrow H_{max}) = \Delta S$, showing the equivalence of the Clausius-Clapeyron equation and the Maxwell relation, provided the latter is only evaluated within the transition field region.

5.5.2 Advanced phenomenological approach: $M(T) \neq$ const.

This model is a generalisation of the previous one. This advanced model includes both the T and H dependences of the magnetisation outside the transition region and the decrease of ΔM with T. The upper panel in Fig. 5.11 shows the modelled $M(T)$ curves at different H. The transition temperature is assumed to shift linearly with the transition field, $dT_t/dH_t \equiv \alpha$=constant. The magnetisation of the low-temperature phase is assumed to decrease linearly with T as $M(T) = \Delta M_0(1-\beta T)$, being zero at the high-temperature phase. The transition between both phases extends within a temperature range $\Delta T_t = \alpha \Delta H_t$, which is assumed to be constant according to the experimental results (see Figs. 5.4 and 5.12 (a)). In this model, $T_t(H)$ is defined for each curve as the temperature at the center of the transition region. As α is considered to be constant, the model should account for the behavior of the entropy change for $0.24 \leq x \leq 0.5$ alloys (see Fig. 5.8 for x=0.45).

The results of the model are compiled in the middle panel in Fig. 5.11. The behaviour, which depends on the temperature range and the maximum applied field, can be summarised as follows :

(i) For temperatures at which the system is in the low-temperature phase ($T \leq T_A$, with $T_A \equiv T_t(H = 0) - \Delta T_t/2$), the entropy change is independent of T and increases linearly with the maximum applied field as

$$\Delta S(0 \rightarrow H_{max}) = -\Delta M_0 \beta H_{max} \quad . \tag{5.4}$$

(ii) In the range $T_A \leq T \leq T_B$ ($T_B \equiv T_t(H = 0) + \Delta T_t/2$), which is the temperature spread of the transition at zero field (see upper panel in Fig. 5.11), the entropy change increases linearly up to $T_t(H_{max}) - \Delta T_t/2$ and reaches a plateau, with a value increasing with H_{max} (see H_1 in Fig. 5.11). The limiting case of this behaviour is obtained when the maximum applied field is strong enough to induce the whole transition (*i.e.*, $H_{max} = \Delta H_t$). Then $T_t(H_{max}) - \Delta T_t/2$ equals T_B and the

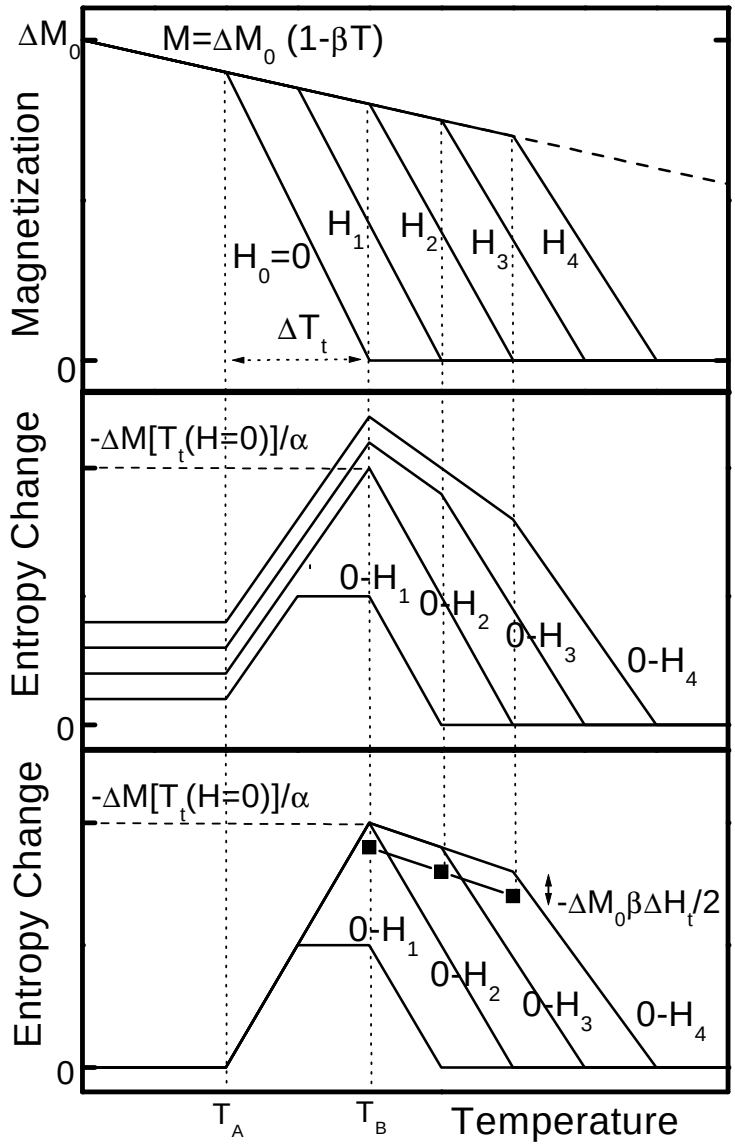

Figure 5.11: Upper panel shows the modelled temperature dependence of the magnetisation across the transition region at different fields, as described for the advanced phenomenological model in the text. Middle panel shows the corresponding entropy change $\Delta S(0 \rightarrow H_{max})$ calculated from the Maxwell relation. Lower panel: Solid lines stand for the entropy change obtained by integrating the Maxwell relation only within the transition region. Connected squares stand for ΔS obtained from the Clausius-Clapeyron equation. The difference between those values is indicated in the Figure.

value is

$$\Delta S\,(0 \rightarrow H_{max}) = -\frac{\Delta M_0[1-\beta T_t(H=0)]}{\alpha} \equiv -\frac{\Delta M[T_t(H=0)]}{\alpha} \qquad (5.5)$$

(see case for H_2 in Fig. 5.11). For higher fields ($H_{max} \geq \Delta H_t$), the transition is also completed at T_B and there is an additional contribution to ΔS due to the field and temperature dependences of M of the low-temperature phase (see cases for H_3 and H_4 in Fig. 5.11). Therefore,

$$\Delta S\,(0 \rightarrow H_{max}) = -\frac{\Delta M[T_t(H=0)]}{\alpha} - \Delta M_0\beta(H_{max}-\Delta H_t)\ . \qquad (5.6)$$

(iii) For temperatures at which the system is in the high-T phase at zero field ($T \geq T_B$) and for low fields (see H_1 and H_2 in Fig. 5.11), ΔS decreases linearly to zero with increasing T, vanishing at $T_t(H_{max}) + \Delta T_t/2$, which corresponds to the minimum temperature at which H_{max} is not enough to start inducing the transition. For fields where the transition is complete (see H_3 and H_4 in Fig. 5.11), ΔS shows plateau-like behavior with a slope $2\Delta M_0\beta/\alpha$ up to $T_t(H_{max}) - \Delta T_t/2$. Above this temperature, the field is not enough to complete the transition and ΔS decreases linearly to zero, vanishing at $T_t(H_{max}) + \Delta T_t/2$.

The lower panel in Fig. 5.11 shows the entropy change (solid lines) calculated by integrating the second term of Eq. 5.1 ($\Delta S\,(H_a \rightarrow H_b)$). The values of ΔS calculated by using the Clausius-Clapeyron equation are also plotted as connected squares. Three main features are to be noted: (i) for temperatures at which the transition does not occur ($T \leq T_A$), $\Delta S\,(0 \rightarrow H_{max})$=0; (ii) for temperatures at which the transition can be completely field-induced ($T \geq T_B$), and for H_{max} strong enough to complete it, the plateau-like regions of all curves overlap, yielding a slope $\Delta M_0\beta/\alpha$; and (iii) ΔS values obtained from the Clausius-Clapeyron equation decrease with the same slope, but lowered by $\delta = \Delta M_0\beta\Delta H_t/2$. The model accounts for the behaviour of the experimental results shown in Fig. 5.12, in Fig. 5.8, and in general for all $0.24 \leq x \leq 0.5$ compounds. We note that in Fig. 5.12 (c) the values of ΔS calculated from the Clausius-Clapeyron equation at low T increase with T due to the fact that, just above the zero-field transition temperature, a fraction of the sample has not yet been transformed to the PM phase and still remains FM [8]. We also note that for $x \leq 0.2$, although α is not constant, the model accounts for the main features of the PM-FM transition. An extension of the present model should consider the dependence of α on H_t and T_t.

In order to improve the model, a linear H dependence of the low-T magnetisation outside the transition region is introduced as $M(T,H) = \Delta M_0(1-\beta T+\gamma H)$. This is a more realistic assumption for the magnetisation curves (Figs. 5.4 and 5.12 (a)). However, the overall behaviour remains unchanged. In this case, Eq.

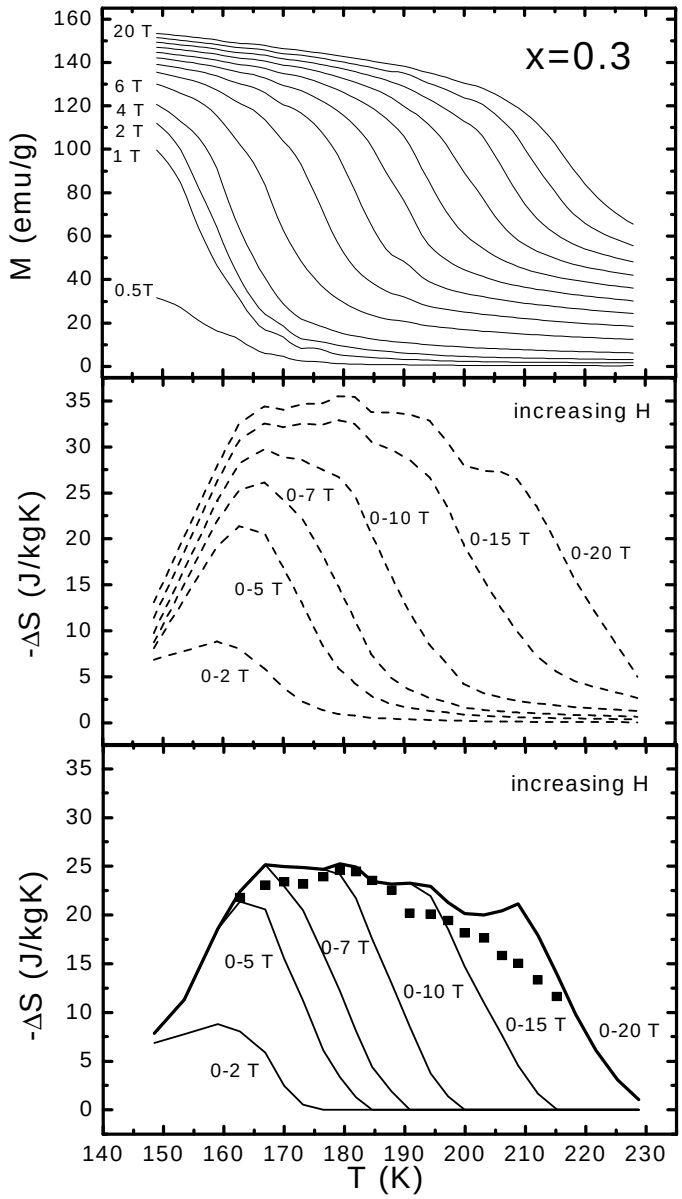

Figure 5.12: Upper panel shows the magnetisation as a function of temperature at different fields (0.5, 1, 2, 4, 6, 8, 10, 12, 14, 16, 18 and 20 T) for x=0.3 compound, taken from $M(H)$ (increasing H) data. Middle panel shows the corresponding entropy change $\Delta S(0 \rightarrow H_{max})$ calculated from the Maxwell relation. Lower panel: Solid lines stand for the entropy change obtained by integrating the Maxwell relation only within the transition region. Connected squares stand for ΔS obtained from the Clausius-Clapeyron equation.

5.5 turns into

$$\Delta S\,(0 \rightarrow H_{max}) = -\frac{\Delta M[T_t(H=0)]}{\alpha} - \frac{\Delta M_0 \gamma \Delta H_t}{2\alpha} \quad , \tag{5.7}$$

the slope of the plateau-like region of ΔS values evaluated within the transition region from the Maxwell relation is now $\Delta M_0 \beta'/\alpha$, with $\beta' = \beta - \gamma/\alpha$, and $\delta' = \Delta M_0 \beta' \Delta H_t/2$. This shift δ' between the Clausius-Clapeyron approach and the Maxwell approach is due to the fact that H heightens T_t, resulting in a reduction of ΔM. Since ΔT_t is assumed to be constant, $\Delta M/\Delta T_t$ in the transition region decreases correspondingly. This H-dependence remains included within the transition region (as $\partial M/\partial T$) and still gives an extra term to the entropy change when calculated from the Maxwell relation by integrating the second term of Eq. 5.1, but does not contribute to the Clausius-Clapeyron equation. Nevertheless, δ' is small for $Gd_5(Si_xGe_{1-x})_4$ alloys. For example, for x=0.45 (see Fig. 5.8), $\Delta M_0\beta'$=0.753 emu/(gK) and ΔH_t ~4 T, yielding δ' ~1.5 J/(kgK), which is within the experimental error of the entropy change. For x=0.3, $\Delta M_0\beta'$=1.163 emu/(gK) and ΔH_t ~7 T, resulting in δ' ~4.1 J/(kgK), which may account for the slight difference observed in Fig. 5.12 (c). Generally, δ' is expected to be small, since it is proportional to the variation of the magnetization outside the transition region and this variation is small in a FM phase. This may be extended to any other field-induced transitions that involve a FM phase.

5.6 Conclusions

The magnetocaloric effect arising from a field variation $0 \rightarrow H_{max}$ can be properly evaluated through the entropy change obtained from the Maxwell method, even when an ideal first-order transition occurs. When the Maxwell relation is evaluated over the whole field range, the T and H dependences of the magnetisation in each phase outside the transition region yield an additional entropy change to that of the actual first-order transition. It has also been shown, from both experimental data and phenomenological models, that the Maxwell relation, the Clausius-Clapeyron equation and the calorimetric measurements yield the entropy change of the first-order magnetostructural transition, provided (i) the Maxwell relation is evaluated only within the field range over which the transition takes place, and (ii) the maximum applied field is high enough to complete the transition. The transition temperature must significantly shift with the applied field, in order to achieve a large MCE taking advantage of the entropy change associated to the first-order transition. This is relevant for the understanding of the thermodynamics and MCE of first-order magnetostructural transitions.

Bibliography

[1] V. K. Pecharsky and K. A. Gschneidner, Jr., Phys. Rev. Lett. **78**, 4494 (1997).

[2] A. Giguère, M. Földeàki, B. Ravi Gopal, R. Chahine, T. K. Bose, A. Frydman, and J. A. Barclay, Phys. Rev. Lett. **83**, 2262 (1999).

[3] K. A. Gschneidner, Jr., V. K. Pecharsky, E. Brück, H. G. M. Duijn, and E. Levin, Phys. Rev. Lett. **85**, 4190 (2000).

[4] J. R. Sun, F. X. Hu, and B. G. Shen, Phys. Rev. Lett. **85**, 4191 (2000).

[5] M. Földeàki, R. Chahine, T. K. Bose, and J. A. Barclay, Phys. Rev. Lett. **85**, 4192 (2000).

[6] V. K. Pecharsky and K. A. Gschneidner, Jr., J. Appl. Phys. **86**, 6315 (1999).

[7] V. K. Pecharsky and K. A. Gschneidner, Jr., Adv. Cryog. Eng. **43**, 1729 (1998).

[8] E. M. Levin, V. K. Pecharsky, and K. A. Gschneidner, Jr., Phys. Rev. B **62**, R14625 (2000).

[9] E. M. Levin, V. K. Pecharsky, K. A. Gschneidner, Jr., and G. J. Miller, Phys. Rev. B **64**, 235103 (2001).

[10] E. M. Levin, K. A. Gschneidner, Jr., and V. K. Pecharsky, Phys. Rev. B **65**, 214427 (2002).

[11] C. Magen, L. Morellon, P. A. Algarabel, C. Marquina, and M. R. Ibarra, J. Phys.: Condens. Matter **15**, 2389 (2003).

[12] A. J. P. Meyer and P. Tanglang, J. Phys. Rad. **14**, 82 (1953).

[13] V. K. Pecharsky and K. A. Gschneidner, Jr., J. Magn. Magn. Mater. **200**, 44 (1999).